MOFs as Emulsifiers Hot Paper

Deutsche Ausgabe: DOI: 10.1002/ange.201602150
Internationale Ausgabe: DOI: 10.1002/anie.201602150

Metal–Organic Framework for Emulsifying Carbon Dioxide and Water

Chengcheng Liu, Jianling Zhang, Lirong Zheng, Jing Zhang, Xinxin Sang, Xinchen Kang, Bingxing Zhang, Tian Luo, Xiuniang Tan, and Buxing Han*

Abstract: *Forming emulsions of carbon dioxide (CO_2) and water can largely expand the utility of CO_2. Herein we propose for the first time the utilization of a metal–organic framework (MOF) for emulsifying CO_2 and water. Owing to the hybrid composition, MOF particles can easily assemble at the CO_2/water interface to create a rigid protective barrier around the dispersed droplet. The MOF-stabilized CO_2 and water emulsion has exceptional stability compared to those emulsions stabilized by surfactants or other solids. Moreover, the CO_2 and water emulsion stabilized by MOF is "tunable" due to the designable features of MOFs and adjustable character of CO_2. Such a novel kind of emulsion composed of CO_2, water, and MOF provides a facile route for constructing MOF superstructures with many advantages. The macroporous networks and hollow capsules of different kinds of MOFs have been successfully derived from CO_2 and water emulsions.*

The utilization of carbon dioxide (CO_2), which is the second-most abundant solvent on earth after water, has attracted much attention.[1–3] CO_2 is generally regarded as a green solvent because it is readily available, inexpensive, nontoxic, nonflammable, has moderate critical temperature and pressure (31.1 °C and 7.38 MPa), and can be easily recaptured and recycled after use. Moreover, CO_2 has adjustable solvent power and excellent mass transfer characteristics that offer many advantages to replace conventional organic solvents.[4–6] However, CO_2 is often a poor solvent because it has no dipole moment, very low dielectric constant and polarizability per volume, which restrict its applications in various fields. To form emulsions of CO_2 and water with the assistance of emulsifiers allows the solubilization of different kinds of compounds within the dispersed phase and continuous phase, which largely expands the utility of CO_2 as a solvent.[7] Moreover, the formation, breakage, and properties of the CO_2 and water emulsions can be easily controlled by the pressure of CO_2. These special properties give CO_2 and water emulsions promising applications in material synthesis[8] and chemical reactions.[9]

[*] C. Liu, Prof. J. Zhang, X. Sang, X. Kang, B. Zhang, T. Luo, X. Tan, Prof. B. Han
Beijing National Laboratory for Molecular Sciences, CAS Key Laboratory of Colloid and Interface and Thermodynamics, Institute of Chemistry, Chinese Academy of Sciences, University of Chinese Academy of Sciences (China)
E-mail: zhangjl@iccas.ac.cn
Dr. L. Zheng, Prof. J. Zhang
Beijing Synchrotron Radiation Facility (BSRF), Institute of High Energy Physics, Chinese Academy of Sciences (China)

Supporting information for this article can be found under: http://dx.doi.org/10.1002/anie.201602150.

The design of amphiphilic (CO_2-philic and hydrophilic) emulsifiers is crucial for the formation of CO_2 and water emulsions. Owing to the poor surfactant-tail solvation caused by the weak van der Waals forces of CO_2, the surfactants for emulsifying CO_2 and water must have low molecular weight, little tail overlap, low free volume at the interface or low cohesive energy densities.[8,10–12] Alternatively, the use of solid particles as emulsifiers can overcome the limitation of poor surfactant-tail solvation, by absorbing at the liquid–liquid interface to create a barrier around the dispersed droplet. Moreover, the solids can be easily separated and recycled by centrifugation or filtration after use. Emulsions stabilized by solids have shown potential applications in, for example, interfacial catalysis,[13] fabrication of superstructures,[14] preparation of Janus colloids.[15] Nevertheless, the strong Hamaker attraction between particles caused by the weak Van der Waals forces of CO_2 often leads to droplet flocculation and coalescence, resulting in poor stability of CO_2 and water emulsion. To overcome this difficulty, the silica/polymeric steric stabilizers[16] or silica particles grafted with various organic ligands[17,18] have been proposed for emulsifying CO_2 and water. Even so, these emulsions can only provide stability against coalescence for hours and so the formation of stable CO_2 and water emulsions remains a severe challenge. Thus there is still a need to develop solid emulsifiers with desirable amphiphilicity to CO_2 and water, resulting from the intrinsic properties of solid particles.

Metal–organic frameworks (MOFs) are a class of crystalline microporous materials constructed by joining metal-containing units with organic linkers,[19,20] which have found wide applications in different fields.[21–25] Importantly, the compositions, structures, and properties of MOFs are easily adjusted by varying the metal ions and organic ligands. Herein we propose for the first time the utilization of MOFs for emulsifying CO_2 and water. The hybrid composition of MOF endows it an amphiphilic properties to assemble at the liquid–liquid interface.[26–28] Such an emulsion consisting of CO_2, water, and MOF is "tunable" due to both the designable features of the MOF emulsifier and adjustable character of solvent CO_2. The experimental results confirm that: 1) the emulsion could be easily prepared by stirring the mixture of water, CO_2, and MOF at room temperature, requiring no additional additives or high-energy input that are usually requisite for emulsifying, 2) the CO_2 and water emulsions are highly stable against coalescence, 3) the morphologies and properties of the emulsions can be easily modulated by the MOF structure and CO_2 pressure. Interestingly, the MOF-stabilized CO_2 and water emulsion provides a unique route for constructing MOF superstructures. The macroporous networks and hollow capsules of different kinds of MOFs were directly obtained from emulsions by removing solvents.

The formation mechanism for the MOF-stabilized emulsion and the derived MOF superstructures is investigated.

For the formation of the water continuous emulsion, $Mn_3(BTC)_2$ (BTC = 1,3,5-benzenetricarboxylate) was synthesized (Figure 1 a,b) and dispersed in water. Then CO_2 was added to the stirred aqueous $Mn_3(BTC)_2$ dispersion at 25 °C. As CO_2 pressure is higher than the vapor pressure of CO_2 (6.4 MPa at 25 °C), a uniform milky-white emulsion was formed (Figure 1 c). The microstructure of the emulsion was identified by electrical conductivity[29] (Figure 1 d). The aqueous dispersion of $Mn_3(BTC)_2$ is highly conductive (ca. 2.4 ms cm^{-1}) because of the partially ionized MOF in water. With the addition of CO_2, the electrical conductivity first increases dramatically, which is caused by the carbonation of dissolved CO_2 in water,[30] and then keeps nearly unchanged (ca. 2.9 ms cm^{-1}). It confirms that the emulsion shown in Figure 1 c corresponds to a CO_2-in-H_2O emulsion, that is, CO_2 droplets are dispersed in water continuous phase. It is notable that the MOF-stabilized emulsion is very stable and no phase separation was observed in at least 6 months after stopping stirring.

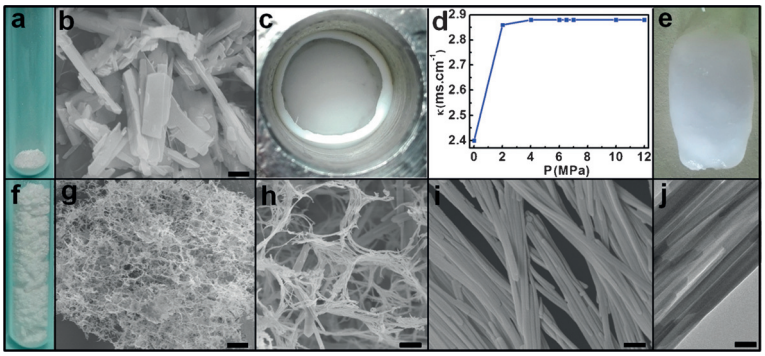

Figure 1. Water-continuous emulsion stabilized by $Mn_3(BTC)_2$ and derivation of the $Mn_3(BTC)_2$ network. a,b) Photograph and SEM image of p-$Mn_3(BTC)_2$. c) Photograph of the emulsion at 7.5 MPa. d) Electrical conductivities of CO_2/H_2O/$Mn_3(BTC)_2$ mixture at different pressures. e) Photograph of the frozen emulsion after releasing CO_2. f)–j) Photograph, SEM, and TEM images of r-$Mn_3(BTC)_2$. Scale bars, 1 μm in (b), 50 μm in (g), 5 μm in (h), 200 nm in (i), and 50 nm in (j).

The CO_2-in-H_2O emulsion provides a novel way for deriving macroporous MOF solid just by removing the liquids. To preserve the microstructure of the emulsion and avoid the macropore collapse during solvent removing process, the emulsion formed at 7.5 MPa was frozen in liquid nitrogen and then CO_2 was released by depressurization. The obtained ice block preserved the morphology of the emulsion (Figure 1 e). Then water was removed by freeze drying and the solid of restructured $Mn_3(BTC)_2$ (r-$Mn_3(BTC)_2$) was obtained. Remarkably, the volume of r-$Mn_3(BTC)_2$ expands tremendously (Figure 1 f) compared with the pristine $Mn_3(BTC)_2$ (p-$Mn_3(BTC)_2$; Figure 1 a). The r-$Mn_3(BTC)_2$ presents a three dimensional network with macropores in the range of 4–30 μm (Figure 1 g), as templated by the CO_2 droplets dispersed in emulsion. Interestingly, the network is assembled from nanofibers of width of 50 nm and length of 15 μm (Figure 1 h–j), much thinner than the p-$Mn_3(BTC)_2$ bars (Figure 1 b). It indicates that the CO_2-in-H_2O emulsion has a dual effect on MOF, that is, downsizing p-$Mn_3(BTC)_2$ to ultrafine nanofibers and conducting their assembly to macroporous network. The r-$Mn_3(BTC)_2$ has a porosity of 87.4 % and total pore volume of 6.98 cm^3 g^{-1}, much higher than those of p-$Mn_3(BTC)_2$ (74.6 % and 2.51 cm^3 g^{-1} for porosity and pore volume, respectively). The CO_2-in-H_2O emulsions stabilized by $Mn_3(BTC)_2$ were also formed at 10.0 MPa and 12.0 MPa, and the macroporous $Mn_3(BTC)_2$ networks made up of ultrafine nanofibers were derived from the emulsions (Figure S1 in the Supporting Information). The r-$Mn_3(BTC)_2$ produced at higher pressure has a larger porosity, which can be attributed to the volume expansion of emulsion at higher CO_2 pressure.

The CO_2 continuous emulsion is more difficult to be stabilized than water continuous emulsion because of thermodynamic and transport limitations for CO_2.[18] Herein we propose the utilization of fluorinated MOF for stabilizing CO_2 continuous emulsion. Mn(hfbba)(3-mepy)(H_2O) (Mn-HFMOF-W) was synthesized using 4,4′-(hexafluoroisopropylidene) bis(benzoic acid) ($C_{17}H_{10}F_6O_4$; H_2hfbba) as the main ligand and 3-methyl pyridine as a coligand[31] (Figure S2). It can emulsify CO_2 and water if the pressure is higher than 6.4 MPa at 25 °C. The emulsion presents dispersive and spherical droplets (Figure 2 c), distinctly different from the CO_2-in-H_2O emulsion which had a uniform milky-white appearance (Figure 1 c). The electrical conductivities of the H_2O/CO_2/Mn-HFMOF-W mixture (Figure 2 d) increase gradually with CO_2 pressure in the lower pressure range, which can be attributed to the acidity of carbonic acid generated by dissolved CO_2 in water.[30] A sharp decrease of conductivity (about 2 orders of magnitude) occurs in the pressure range of

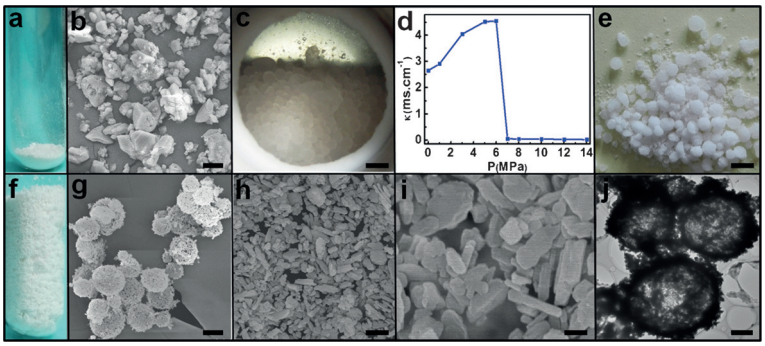

Figure 2. CO_2 continuous emulsion stabilized by Mn-HFMOF-W and derivation of Mn-HFMOF-W capsules. a,b) Photograph and SEM image of p-Mn-HFMOF-W. c) Photograph of the emulsion at 7.5 MPa. d) Electrical conductivities of CO_2/H_2O/Mn-HFMOF-W mixture at different CO_2 pressures. e) Photograph of the frozen emulsion after releasing CO_2. f)–j) Photograph, SEM and TEM images of r-Mn-HFMOF-W. Scale bars, 10 μm in (b), 2 mm in (c), 300 μm in (e), 15 μm in (g), 1.5 μm in (h), 300 nm in (i), 3 μm in (j).

6.0–7.0 MPa and then the conductivity drops to essentially zero at higher pressure, indicating non-conducting CO_2 is the continuous phase of emulsion. Further, the emulsion was dyed with hydrophilic indicator methyl orange and the result confirms that water droplets are dispersed in continuous CO_2 (Figure S3). The emulsion is highly stable and no phase separation was observed over at least 6 months. The restructured Mn-HFMOF-W (r-Mn-HFMOF-W) derived from the emulsion has hollow micron-sized capsules (Figure 2 f–h), which are assembled by nanoparticles of the size of hundreds of nanometers (Figure 2 i,j). In comparison with the irregular agglomerates of p-Mn-HFMOF-W in microns (Figure 2 b), it is evident that the emulsion can not only downsize p-Mn-HFMOF-W to ultrafine nanoparticles but also conduct their assembly to hollow capsules. The Mn-HFMOF-W-stabilized emulsions were also formed at 10.0 MPa and 12.0 MPa (Figure S4). The droplet size of the emulsion decreases with increasing pressure, resulting from lower interfacial tension at higher pressure.[32,33] The Mn-HFMOF-W capsules assembled by ultrafine nanoparticles were synthesized from the emulsions (Figure S5).

By comparison of Figure 2 c,e,g, it is interesting to find that the size of r-Mn-HFMOF-W capsules is much smaller than that of the emulsion droplets. Since r-Mn-HFMOF-W capsules are templated by emulsion droplets, such a decrease by orders of magnitude is abnormal. It attracts our attention to further investigate the droplet microstructure of the emulsion. Owing to the high pressure, the CO_2 and water emulsion cannot be characterized in situ by conventional techniques. In this case one of the ice particles in Figure 2 e was picked up (Figure 3 a) and characterized separately by optical microscope photograph. A secondary structure was observed in the single ice particle (Figure 3 b). Moreover, the single ice particle was dried separately and the solid obtained (Figure 3 c) presents hundreds of hollow capsules assembled by nanoparticles (Figure 3 d,e). It indicates that in the emulsion, one droplet contains lots of inner droplets of much smaller size. To get further evidence, the emulsion stabilized by Mn-HFMOF-W was dyed by a fluorescent indicator Rhodamine B, then frozen. One frozen ice particle was dried separately and the dyed Mn-HFMOF-W particle was characterized by confocal laser scanning microscopy (CLSM) image. Figure 3 f–h clearly shows that many dyed hollow capsules are included inside the single particle, further proving the formation of multiple CO_2-in-H_2O-in-CO_2 emulsion stabilized by Mn-HFMOF-W.

The possibilities of emulsifying CO_2 and water with other MOFs were investigated. $Cu_3(BTC)_2$ can stabilize the CO_2-in-H_2O emulsion (Figure S6), while the fluorinated MOF Co(hfbba)(3-mepy)(H_2O) (Co-HFMOF-W) stabilizes the CO_2-in-H_2O-in-CO_2 emulsion similar to that stabilized by Mn-HFMOF-W (Figure S7). After removing solvents, the macroporous $Cu_3(BTC)_2$ network and Co-HFMOF-W hollow capsules were obtained, which are both assembled by nanoparticles (Figure S6,S7). Compared with the p-MOFs, r-$Cu_3(BTC)_2$, and r-Co-HFMOF-W have significantly lower densities and significantly increased porosities and pore volumes (Table 1). The results confirm that MOFs are versatile in emulsifying water and CO_2 to form different emulsions, which provide a promising way for producing MOF superstructures with tunable properties.

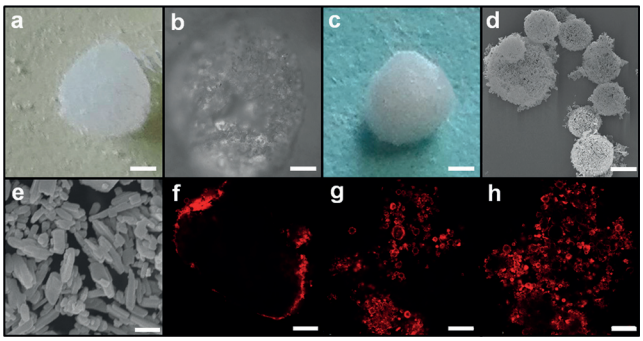

Figure 3. Characterization of multiple the CO_2-in-H_2O-in-CO_2 emulsion stabilized by Mn-HFMOF-W. a,b) Photograph and optical microscope photograph of one frozen droplet from Figure 2 e. c)–e) Photograph and SEM images of one dried droplet. f)–h) CLSM images of one dried droplet dyed with Rhodamine B. Scale bars, 1 mm in (a), 200 μm in (b), 1 mm in (c), 15 μm in (d), 300 nm in (e), 200 μm in (f), 100 μm in (g), 100 μm in (h).

The hydrophilicity of the four MOFs was measured through aqueous phase by static contact-angle instrument. $Mn_3(BTC)_2$ and $Cu_3(BTC)_2$ particles have contact angles much less than 90° (Figure 4 a,b), indicating a strong hydrophilicity. Hence the water–CO_2 interface stabilized by $Mn_3(BTC)_2$ and $Cu_3(BTC)_2$ particles bends around CO_2 phase, leading to the formation of CO_2-in-H_2O emulsion (Figure 4 e,f). Conversely, the Mn-HFMOF-W and Co-HFMOF-W particles with contact angles greater than 90° (Figure 4 c,d) are less hydrophilic and more CO_2-philic owing to the fluoric ligand,[31] favoring the formation of CO_2 continuous emulsion. However, the above results show that the multiple CO_2-in-H_2O-in-CO_2 emulsion is formed with the aid of Mn-HFMOF-W (Figure 4 g). It is well established that forming a multiple emulsion is usually difficult and requires two kinds of surfactants,[34] two-step emulsification process,[35] high energy input[36] or utilization of specially designed facilities.[37]

Table 1: Morphologies, densities and porosity properties of the pristine MOFs (p-MOFs) and the restructured MOFs (r-MOFs).

MOFs	Morphology	Density [$g\,cm^{-3}$]	Porosity [%]	V_{pore} [$cm^3\,g^{-1}$]
p-$Mn_3(BTC)_2$	bars	0.372	74.6	2.51
r-$Mn_3(BTC)_2$	network	0.018	87.4	6.98
p-$Cu_3(BTC)_2$	agglomerates	0.335	75.4	2.20
r-$Cu_3(BTC)_2$	network	0.022	86.9	6.87
p-Mn-HFMOF-W	agglomerates	0.468	50.1	1.08
r-Mn-HFMOF-W	capsules	0.025	74.0	3.71
p-Co-HFMOF-W	agglomerates	0.370	69.8	1.98
r-Co-HFMOF-W	capsules	0.021	74.6	3.13

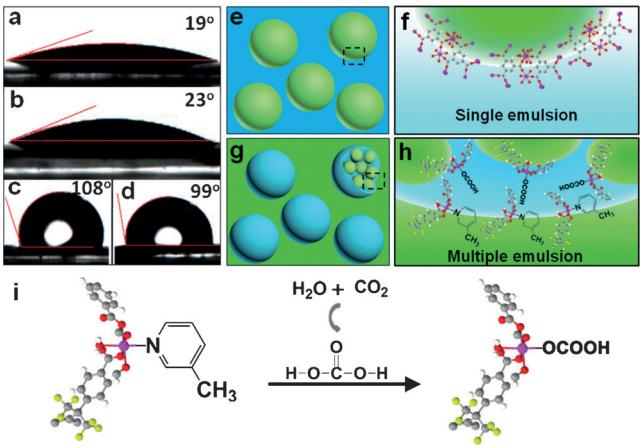

Figure 4. Mechanism studies on the emulsions stabilized by different MOFs. a)–d) Contact angles of a) $Mn_3(BTC)_2$, b) $Cu_3(BTC)_2$, c) Mn-HFMOF-W, and d) Co-HFMOF-W with H_2O droplets. e),f) CO_2-in-H_2O emulsion stabilized by $Mn_3(BTC)_2$ at interface. g,h) CO_2-in-H_2O-in-CO_2 emulsion stabilized by Mn-HFMOF-W at interface. i) Mechanism of the ligand substitution.

Herein the multiple emulsion can be attained simply by stirring the mixture of CO_2, water and Mn-HFMOF-W at room temperature. The formation mechanism for the multiple emulsion was investigated by FT-IR spectra, X-ray photoelectron spectroscopy, X-ray absorption spectroscopy, elemental analysis and inductively coupled plasma optical emission spectrometer (see detailed discussion in Figures S10–14 and Table S1). All the results reveal that the coligand 3-methyl pyridine of p-Mn-HFMOF-W is partially substituted by carbonic acid during restructuring process in emulsion, as illustrated in Figure 4i. The Mn-HFMOF-W without ligand substitution is more CO_2-philic and absorbs at the outer CO_2-water interface, while the Mn-HFMOF-W with ligand substitution by carbonic acid is more hydrophilic and distributes at the inner water–CO_2 interface (Figure 4h). Therefore, the multiple CO_2-in-H_2O-in-CO_2 emulsion that the water droplets dispersed in CO_2 contain some smaller inner CO_2 droplets is stabilized with the cooperation of the two MOFs.

The experimental results show that the CO_2 and water emulsion has a dual effect on MOF, 1) downsizing the pristine MOFs to ultrafine nanocrystals, and 2) conducting the assembly of these nanocrystals to superstructures. The mechanism of downsizing effect of emulsion on the MOF is very interesting. It has been recognized that high-pressure CO_2 favors the formation of ultrafine particles by the viscosity-lowering effect.[38] Herein, to detect whether high-pressure CO_2 is relevant to the MOF fragmentation, p-$Mn_3(BTC)_2$ and p-Mn-HFMOF-W were dispersed in liquid CO_2 at 7.5 MPa and 25 °C for 2 h. No morphological difference was found for the as-treated MOFs as compared with the pristine MOFs (Figure S15), indicating that the MOF fragmentation is nothing to do with the high-pressure CO_2. Further, the effect of the acidity change caused by the carbonation of dissolved CO_2 in water was investigated by dispersing the pristine MOFs in HCl aqueous solution (pH 3) at 25 °C for 2 h. Rods with diameters of hundreds of nanometers were obtained for $Mn_3(BTC)_2$, which are much thicker than the r-$Mn_3(BTC)_2$ obtained from emulsion (50 nm); the as-treated Mn-HFMOF-W remains in the same morphology as p-Mn-HFMOF-W (Figure S16). These results reveal that the acidity change is not relevant for MOF fragmentation. It is well established that the formation of emulsion induces the fast creation of new interfaces .[39] The immense interface caters for MOF fragmentation,[40] which in turn can stabilize the emulsion in a better fashion. Therefore, the MOFs are downsized during the emulsification process to produce nanocrystals (e.g. $Mn_3(BTC)_2$ nanofibers and Mn-HFMOF-W nanoparticles).

Based on the above results, a possible mechanism for constructing MOF superstructures in CO_2 and water emulsions is proposed in Scheme 1. For the hydrophilic MOF (e.g. $Mn_3(BTC)_2$), the MOF nanofibers adsorbed at CO_2–water interface are probably contiguous with those dispersed in water continuous phase (Scheme 1b). After removing solvents, the MOF nanofibers are crosslinked into a 3D network with a macroporous structure templated by CO_2 droplets (Scheme 1c). For the fluorinated MOF (e.g. Mn-HFMOF-W), the multiple CO_2-in-H_2O-in-CO_2 emulsion is formed. Each water droplet dispersed in CO_2 (Scheme 1e) contains some smaller inner CO_2 droplets (Scheme 1f). The ultrafine MOF nanoparticles are easily adsorbed at the CO_2–water interface, forming a dense film (monolayer or multilayer) around the droplets to stabilize them. Therefore, the hollow MOF capsules assembled by nanoparticles are produced from the multiple emulsion after removing solvents (Scheme 1g).

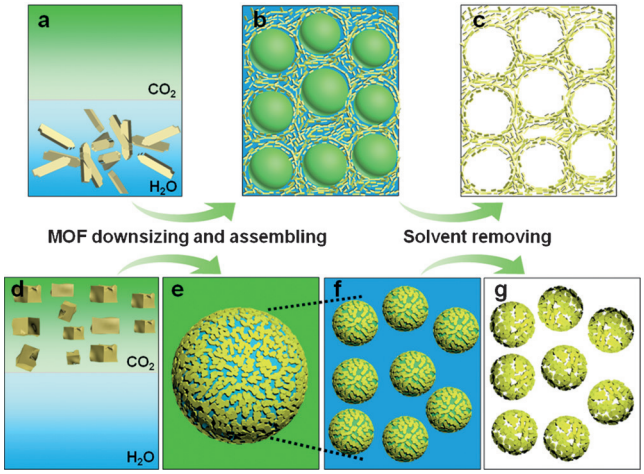

Scheme 1. Schematic illustration for constructing MOF superstructures in CO_2 and water emulsions. a)–c) Derivation of macroporous MOF network assembled by nanofibers from a CO_2-in-H_2O emulsion. d)–g) Derivation of MOF capsules assembled by nanoparticles from CO_2-in-H_2O-in-CO_2 emulsion.

In conclusion, we demonstrate for the first time that CO_2 and water emulsions are stabilized by MOFs. The emulsion could be easily prepared by stirring the mixture of water, CO_2, and MOF at room temperature and is highly stabile against coalescence. The MOF nanocrystals assembled at the CO_2–water interface create a rigid protective barrier around

dispersed droplet, thus inhibiting droplet coalescence effectively. Moreover, the emulsion is "tunable" as a result of to both the variability associated with MOFs which are uses as the emulsifier and the adjustable character of solvent CO_2. This novel kind of emulsion provides a unique way for producing MOF superstructures. The macroporous network and hollow capsules assembled by ultrafine MOF nanocrystals were directly obtained from emulsions after releasing solvents. We anticipate that the CO_2 and water emulsions stabilized by MOFs may be utilized in the in situ synthesis of MOF composites, for example, MOF/MOF, MOF/polymer, MOF/metal, MOF/metal oxide. It is also promising to find their potential applications in other fields, for example, chemical reaction, deposition.

Acknowledgements

We thank the National Natural Science Foundation of China (21525316, 21133009, U1232203, 21021003), Chinese Academy of Sciences (KJCX2.YW.H16).

Keywords: CO_2 · emulsions · H_2O · metal–organic frameworks · superstructures

How to cite: *Angew. Chem. Int. Ed.* **2016**, *55*, 11372–11376
Angew. Chem. **2016**, *128*, 11544–11548

[1] S. Gao, Y. Lin, X. C. Jiao, Y. F. Sun, Q. Q. Luo, W. H. Zhang, D. Q. Li, J. L. Yang, Y. Xie, *Nature* **2016**, *529*, 68–71.
[2] C. C. Hwang, J. J. Tour, C. Kittrell, L. Espinal, L. B. Alemany, J. M. Tour, *Nat. Commun.* **2014**, *5*, 3961.
[3] G. A. Olah, G. K. S. Prakash, A. Goeppert, *J. Am. Chem. Soc.* **2011**, *133*, 12881–12898.
[4] J. L. Zhang, B. X. Han, *Acc. Chem. Res.* **2013**, *46*, 425–433.
[5] A. Caballero, E. Despagnet-Ayoub, M. M. Díaz-Requejo, A. Díaz-Rodríguez, M. E. González-Núñez, R. Mello, B. K. Muñoz, W. S. Ojo, G. Asensio, M. Etienne, P. J. Pérez, *Science* **2011**, *332*, 835–838.
[6] J. Jennings, M. Beija, A. P. Richez, S. D. Cooper, P. E. Mignot, K. J. Thurecht, K. S. Jack, S. M. Howdle, *J. Am. Chem. Soc.* **2012**, *134*, 4772–4781.
[7] K. P. Johnston, S. R. P. da Rocha, *J. Supercrit. Fluids* **2009**, *47*, 523–530.
[8] B. Tan, A. I. Cooper, *J. Am. Chem. Soc.* **2005**, *127*, 8938–8939.
[9] S. M. Cenci, L. R. Cox, G. A. Leeke, *ACS Sustainable Chem. Eng.* **2014**, *2*, 1280–1288.
[10] M. T. Stone, P. G. Smith, S. R. P. da Rocha, P. J. Rossky, K. P. Johnston, *J. Phys. Chem. B* **2004**, *108*, 1962–1966.
[11] W. Ryoo, S. E. Webber, R. T. Bonnecaze, K. P. Johnston, *Langmuir* **2006**, *22*, 1006–1015.
[12] J. Eastoe, S. Gold, D. C. Steytler, *Langmuir* **2006**, *22*, 9832–9842.
[13] Z. W. Chen, H. W. Ji, C. Q. Zhao, E. G. Ju, J. S. Ren, X. G. Qu, *Angew. Chem. Int. Ed.* **2015**, *54*, 4904–4908; *Angew. Chem.* **2015**, *127*, 4986–4990.
[14] M. L. Pang, A. J. Cairns, Y. L. Liu, Y. Belmabkhout, H. C. Zeng, M. Eddaoudi, *J. Am. Chem. Soc.* **2013**, *135*, 10234–10237.
[15] B. Liu, W. Wei, X. Z. Qu, Z. H. Yang, *Angew. Chem. Int. Ed.* **2008**, *47*, 3973–3975; *Angew. Chem.* **2008**, *120*, 4037–4039.
[16] L. Calvo, J. D. Holmes, M. Z. Yates, K. P. Johnston, *J. Supercrit. Fluids* **2000**, *16*, 247–260.
[17] A. J. Worthen, H. G. Bagaria, Y. S. Chen, S. L. Bryant, C. Huh, K. P. Johnston, *J. Colloid Interface Sci.* **2013**, *391*, 142–151.
[18] S. S. Adkins, D. Gohil, J. L. Dickson, S. E. Webber, K. P. Johnston, *Phys. Chem. Chem. Phys.* **2007**, *9*, 6333–6343.
[19] H. Furukawa, K. E. Cordova, M. O'Keeffe, O. M. Yaghi, *Science* **2013**, *341*, 974.
[20] O. M. Yaghi, M. O'Keeffe, N. W. Ockwig, H. K. Chae, M. Eddaoudi, J. Kim, *Nature* **2003**, *423*, 705–714.
[21] T. M. McDonald, J. A. Mason, X. Q. Kong, E. D. Bloch, D. Gygi, A. Dani, V. Crocella, F. Giordanino, S. O. Odoh, W. S. Drisdell, B. Vlaisavljevich, A. L. Dzubak, R. Poloni, S. K. Schnell, N. Planas, K. Lee, T. Pascal, L. W. F. Wan, D. Prendergast, J. B. Neaton, B. Smit, J. B. Kortright, L. Gagliardi, S. Bordiga, J. A. Reimer, J. R. Long, *Nature* **2015**, *519*, 303–308.
[22] O. K. Farha, A. O. Yazaydin, I. Eryazici, C. D. Malliakas, B. G. Hauser, M. G. Kanatzidis, S. T. Nguyen, R. Q. Snurr, J. T. Hupp, *Nat. Chem.* **2010**, *2*, 944–948.
[23] Z. Huang, P. S. White, M. Brookhart, *Nature* **2010**, *465*, 598–601.
[24] J. Huo, M. Marcello, A. Garai, D. Bradshaw, *Adv. Mater.* **2013**, *25*, 2717–2722.
[25] R. Sabouni, H. G. Gomaa, *Soft Matter* **2015**, *11*, 4507–4516.
[26] B. Xiao, Q. Yuan, R. A. Williams, *Chem. Commun.* **2013**, *49*, 8208–8210.
[27] J. Park, D. Q. Yuan, K. T. Pham, J. R. Li, A. Yakovenko, H. C. Zhou, *J. Am. Chem. Soc.* **2012**, *134*, 99–102.
[28] H. S. Cho, H. X. Deng, K. Miyasaka, Z. Y. Dong, M. Cho, A. V. Neimark, J. K. Kang, O. M. Yaghi, O. Terasaki, *Nature* **2015**, *527*, 503–507.
[29] J. L. Zhang, B. X. Han, Y. J. Zhao, W. Li, Y. H. Liu, *Phys. Chem. Chem. Phys.* **2011**, *13*, 6065–6070.
[30] D. X. Liu, J. L. Zhang, B. X. Han, J. F. Fan, T. C. Mu, Z. M. Liu, W. Z. Wu, J. Chen, *J. Chem. Phys.* **2003**, *119*, 4873–4878.
[31] P. Pachfule, R. Das, P. Poddar, R. Banerjee, *Inorg. Chem.* **2011**, *50*, 3855–3865.
[32] S. R. P. da Rocha, J. Dickson, D. M. Cho, P. J. Rossky, K. P. Johnston, *Langmuir* **2003**, *19*, 3114–3120.
[33] Y. S. Chen, A. S. Elhag, L. Y. Cui, A. J. Worthen, P. P. Reddy, J. A. Noguera, A. M. Ou, K. Ma, M. Puerto, G. J. Hirasaki, Q. P. Nguyen, S. L. Biswal, K. P. Johnston, *Ind. Eng. Chem. Res.* **2015**, *54*, 4252–4263.
[34] F. Michaut, P. Perrin, P. Hebraud, *Langmuir* **2004**, *20*, 8576–8581.
[35] B. P. Binks, A. K. F. Dyab, P. D. I. Fletcher, *Chem. Commun.* **2003**, 2540–2541.
[36] J. A. Hanson, C. B. Chang, S. M. Graves, Z. Li, T. G. Mason, T. J. Deming, *Nature* **2008**, *455*, 85–88.
[37] H. C. Shum, J. W. Kim, D. A. Weitz, *J. Am. Chem. Soc.* **2008**, *130*, 9543–9549.
[38] L. Peng, J. L. Zhang, Z. M. Xue, B. X. Han, X. X. Sang, C. C. Liu, G. Y. Yang, *Nat. Commun.* **2014**, *5*, 5465.
[39] A. Javadi, N. Mucic, M. Karbaschi, J. Y. Won, M. Lotfi, A. Dan, V. Ulaganathan, G. Gochev, A. V. Makievski, V. I. Kovalchuk, N. M. Kovalchuk, J. Kragel, R. Miller, *Eur. Phys. J.: Spec. Top.* **2013**, *222*, 7–29.
[40] N. Wang, Q. Xu, S. S. Xu, Y. H. Qi, M. Chen, H. X. Li, B. X. Han, *Sci. Rep.* **2015**, *5*, 16764.

Received: March 2, 2016
Revised: April 28, 2016
Published online: August 16, 2016

